

Dalton Transactions

An international journal of inorganic chemistry

Accepted Manuscript

This article can be cited before page numbers have been issued, to do this please use: M. Hill, K. Pearce, H. Liu and C. L. McMullin, *Dalton Trans.*, 2026, DOI: 10.1039/D6DT01406B.



This is an Accepted Manuscript, which has been through the Royal Society of Chemistry peer review process and has been accepted for publication.

Accepted Manuscripts are published online shortly after acceptance, before technical editing, formatting and proof reading. Using this free service, authors can make their results available to the community, in citable form, before we publish the edited article. We will replace this Accepted Manuscript with the edited and formatted Advance Article as soon as it is available.

You can find more information about Accepted Manuscripts in the [Information for Authors](#).

Please note that technical editing may introduce minor changes to the text and/or graphics, which may alter content. The journal's standard [Terms & Conditions](#) and the [Ethical guidelines](#) still apply. In no event shall the Royal Society of Chemistry be held responsible for any errors or omissions in this Accepted Manuscript or any consequences arising from the use of any information it contains.

COMMUNICATION

A Strontium Alumanyl

Kyle G. Pearce, Han-Ying Liu, Claire L. McMullin* and Michael S. Hill*

Received 00th January 20xx,
Accepted 00th January 20xx

DOI: 10.1039/x0xx00000x

The strontium alumanyl, $[(\text{BDI})\text{SrAl}(\text{SiN}^{\text{Dipp}})]$, has been prepared from $[(\text{BDI})\text{Sr}(\text{BPh}_4)]$ and $[(\text{SiN}^{\text{Dipp}})\text{AlK}]_2$. Like its previously described calcium analogue, structural and computational analysis indicates that the Sr-Al interaction is only marginally involved in the engagement of the Sr cation and alumanyl anion. Unlike its lighter equivalent, however, $[(\text{BDI})\text{SrAl}(\text{SiN}^{\text{Dipp}})]$ does not react with THF, the presence of which only appears to enhance its presumed dismutation and reaction with the toluene solvent at 100 °C to provide a strontium bis-hydrido(*meta*-tolyl)aluminate.

The pursuit of heterometal-to-group 13 element bonds has been substantially assisted by anions of the form $[\text{R}_2\text{E}]^-$ ($\text{E} = \text{B},^1 \text{Al},^{2-5} \text{Ga},^{6,7} \text{In}^{8,9}$). Especially notable is the recent progress when $\text{E} = \text{Al}$, where alumanyl anions have now been used to generate a plethora of previously inaccessible heterobimetallic species.¹⁰⁻²⁵ Beyond sheer synthetic novelty, such studies highlight a potential for cooperative reactivity afforded by the dissimilar metal centres. An apposite case in point is, thus, provided by the wide range of group 1 alumanyls that have been described since Goicoechea and Aldridge's seminal report of the potassium derivative, $[(^{\text{xanth}}\text{NON})\text{AlK}]_2$ ($^{\text{xanth}}\text{NON} = 4,5\text{-bis}(2,6\text{-diisopropylanilido})\text{-}2,7\text{-di-}t\text{-tert-butyl-}9,9\text{-dimethylxanthene}$ (**1**; Figure 1).^{12,26-33} While all such species display high nucleophilicity and reducing potential at their formal Al(I) centres, more subtle gradations in reactivity may also be ascribed to the identity of the accompanying alkali metal cation. Our own observations of $[(\text{SiN}^{\text{Dipp}})\text{AlM}]_2$ (**2^M**; Figure 1 where $\text{M} = \text{Li}, \text{Na}, \text{K}, \text{Rb}, \text{Cs}$; $\text{SiN}^{\text{Dipp}} = (\text{CH}_2\text{SiMe}_2\text{NDipp})_2$, $\text{Dipp} = 2,6\text{-diisopropylphenyl}$) have,^{28,34,35} for example, highlighted a variable competence for C-H oxidative addition of benzene and π -basic substrates traceable to the relative facility for substrate π -engagement with the M^+ cations.^{35,36}

Department of Chemistry, University of Bath, Claverton Down, Bath, BA2 7AY, UK.

Supplementary Information available: Experimental procedures and characterisation data for all new compounds. Full details of computational studies. Crystal data, details of data collections and refinements. CCDC numbers: 2548846-2548848. See DOI: XXXX

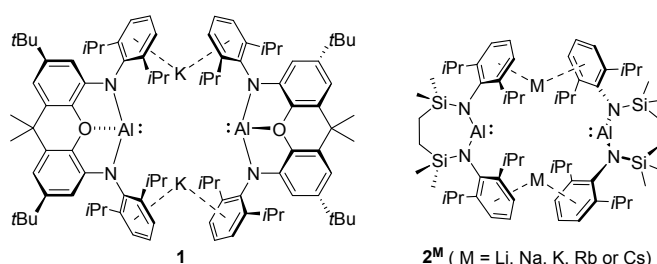
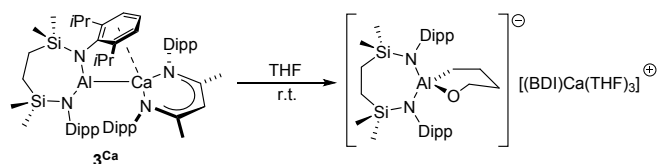


Figure 1. Structures of compounds **1** and **2^M**.

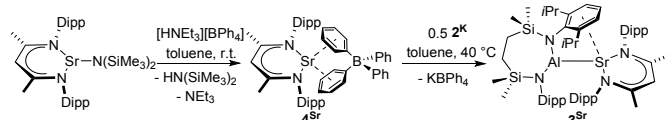
Although examples are limited to the lighter metals of the series, studies of alkaline earth (Ae) alumanyls infer that similar variations in chemistry may prevail down group 2. Both the unique beryllium species, $[(^{\text{xanth}}\text{NON})\text{AlBeCp}]$,³⁷ and a handful of derivatives in which a magnesium centre is further coordinated by β -diketimate anions comprise terminal Ae-Al interactions.^{26,28,32,38} In contrast, the calcium complex, $[(\text{BDI})\text{CaAl}(\text{SiN}^{\text{Dipp}})]$ (**3^{Ca}**, Scheme 1; $\text{BDI} = \text{HC}\{(\text{Me})\text{CNDipp}\}_2$), exhibited an Al-Ca separation [3.1664(4) Å] that is 6.6% longer than the sum of the covalent radii of the constituent metals and a calcium coordination sphere augmented by η^6 -engagement with a Dipp substituent of the Al-coordinated diamide ligand (Ca-C range 2.9709(17) – 3.2215(15) Å).²⁸ Computational (QTAIM) assessment of the Al-Ae interactions of **3^{Ca}** and its magnesium analogue (**3^{Mg}**) identified bond critical points (BCPs) with positive Laplacians (**3^{Mg}** +0.033; **3^{Ca}** +0.020 ea_0^{-5}) characteristic of interactions that are largely electrostatic in origin. Although the interaction between the calcium centre and the Dipp π -system was judged to be largely non-covalent and only weakly stabilising of the structure, initial studies also highlighted significantly divergent reactivity for **3^{Ca}**. For example, whereas **3^{Mg}** was stable in ether solvents, addition of THF to **3^{Ca}** resulted in the immediate generation of a charge separated species, $[(\text{BDI})\text{Ca}(\text{THF})_3]^+[(\text{SiN}^{\text{Dipp}})\text{Al}\{\text{O}(\text{CH}_2)_4\}]^-$, comprising an aluminate product of C-O oxidative addition to the Al(I) centre of the $[(\text{SiN}^{\text{Dipp}})\text{Al}]^-$ anion (Scheme 1).²⁸





Scheme 1. The structure of **3^{Ca}** and its reaction with THF.

Beyond such differences, the isolation of both **3^{Mg}** and **3^{Ca}** highlight the long-standing utility of the BDI anion for exploration of the coordination chemistry of the lighter alkaline earth elements.^{39–43} Detailed studies of even calcium derivatives, however, have long been bedevilled by a propensity toward irreversible Schlenk-type solution redistribution to homoleptic species, behaviour exacerbated for increasingly labile heteroleptic compounds of the heaviest members of the series, Sr and Ba.^{43,44} While this reactivity may be suppressed by more sterically demanding variants of the β -diketiminato structure,^{45–47} the introduction of bulkier *N*-aryl substituents would also introduce a significant perturbation to an otherwise isoelectronic series of compounds and undermine coherent comparison to **3^{Mg}** and **3^{Ca}**. It is notable, therefore, that the synthesis of both **3^{Mg}** and **3^{Ca}** utilised the tetraphenylborate starting materials, [(BDI)Ae(BPh₄)] (**4^{Mg}** Ae = Mg; **4^{Ca}** Ae = Ca), in metathesis reactions with [(SiN^{Dipp})AlK]₂. While not a central consideration at the time of its report,²⁸ the monomeric species **4^{Ca}** proved notably stable to Schlenk-type redistribution, a durability that may be plausibly ascribed to the twofold Ca $\cdots\mu$ - η^6 -(Ph)₂BPh₂ arene interactions with the [BPh₄][−] anion that further encapsulate the calcium centre. Similar π -engagement is slowly emerging as a general feature of heavier alkaline earth behaviour.^{48–55} In an extension of this chemistry, therefore, we report here that an alumanyl derivative of strontium is accessible via an analogous tetraphenylborate derivative, [(BDI)Sr(BPh₄)] (**4^{Sr}**), without any additional enhancement of the steric demands of the supporting BDI ligand.



Scheme 2. Synthesis of compounds **4^{Sr}** and **3^{Sr}**.

Compound **4^{Sr}** was synthesised in high yield (80%) in an analogous fashion to its lighter metal congeners by addition of [HNEt₃][BPh₄] to a toluene solution of [(BDI)SrN(SiMe₃)₂] (Scheme 2) and was fully characterised by ¹H, ¹³C and ¹¹B ($\delta^{11}\text{B} = -4.8$ ppm) NMR spectroscopy in *d*₈-toluene and single crystal X-ray diffraction.⁵⁶ **4^{Sr}** was notably stable toward its dismutation to [(BDI)₂Sr] in solution at ambient temperature and the results of the solid-state analysis confirmed its constitution as a mononuclear strontium species in which the coordination sphere of the alkaline earth centre is stabilised by a combination of the BDI chelate and twofold Sr $\cdots\mu$ - η^6 -(Ph)₂BPh₂ arene interactions with the borate anion (Figure S21).

Addition of a half molar equivalent of **2^K** to **4^{Sr}** in toluene generated an orange solution and an off-white precipitate, presumed to be KBPh₄, filtration and crystallisation of which provided a moderate yield of **3^{Sr}** (50%) as amber coloured single crystals suitable for X-ray analysis (Scheme 2). Like its calcium alumanyl analogue (**3^{Ca}**), the structure of **3^{Sr}** displays an aluminium-to-alkaline earth separation [Sr1–Al1 3.2953(4) Å] that is significantly longer than the sum of the covalent radii of the metal centres [3.16 Å] (Figure 2). In a similar manner to that observed in **3^{Ca}**, the engagement of the alumanyl anion with Sr1 is augmented by an η^6 -interaction of the C36–C41-containing Dipp substituent of the aluminium-coordinated (SiN^{Dipp}) ligand (Sr \cdots C_{cent} 2.915 Å). The resultant asymmetry in the relative disposition of the {(SiN^{Dipp})Al} and {(BDI)Sr} moieties is, thus, reflected by the significant discrepancy in the N3–Al1–Sr1 [96.96(3)°] and N4–Al1–Sr1 [152.22(4)°] angles subtended at the alumanyl centre.

DFT electronic structure calculations of **3^{Sr}** (BP86/BS2, see ESI for full methodology details) revealed similarities to **3^{Ca}**, specifically in the QTAIM plot where a bond path was identified between Sr and Al (Figure 3a), with a minute reduction in electron density at the bond critical point (BCP); $\rho(r) = 0.019$ (**3^{Sr}**), 0.020 (**3^{Ca}**) and $\nabla^2\rho(r) = +0.019$ (**3^{Sr}**), +0.020 (**3^{Ca}**). These data suggest that the Sr–Al interaction is weakly ionic in nature, confirmed by a small positive Laplacian ($\nabla^2\rho(r)$) value, though a modicum of covalency could be interpreted from the negative H(*r*) value. A bond path was also identified between Sr and the *para* carbon of a Dipp substituent of the (SiN^{Dipp}) ligand framework supporting the alumanyl. Similar attributes were ascribed to the analogous BCP identified in **3^{Ca}**, again indicating that the Ae–C_a bond paths are effectively identical.

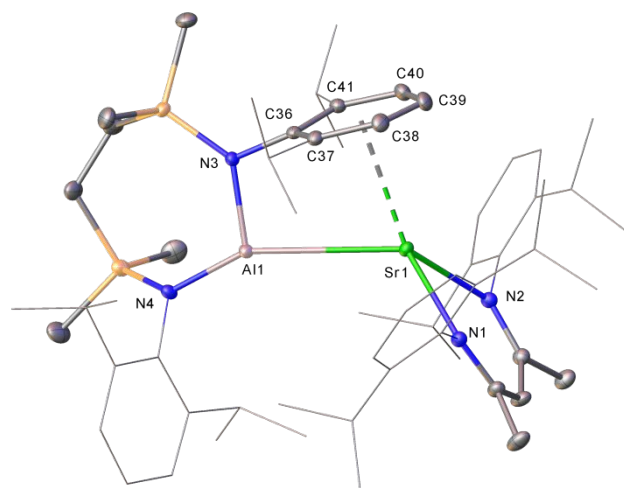


Figure 2. Molecular structure of compound **3^{Sr}** with displacement ellipsoids at 30%. For clarity, hydrogen atoms and an occluded but disordered molecule of toluene solvent are omitted. Similarly, Dipp substituents not involved in π \cdots arene interactions and all *iso*-propyl substituents are displayed as wireframe. Selected bond lengths (Å) and angles (°): Sr1–Al1 3.2953(4), Sr1–N2 2.5009(10), Sr1–N1 2.4986(10), Al1–N3 1.9034(10), Al1–N4 1.8516(11), N1–Sr1–N2 73.97(3), N3–Al1–N4 109.97(5), N1–Sr1–Al1 119.45(2), N2–Sr1–Al1 125.00(2), N3–Al1–Sr1 96.96(3), N4–Al1–Sr1 152.22(4).



Natural Bond Orbital (NBO) analysis of **3^{Sr}** gives a Wiberg Bond Index of 0.454 between the Al and Sr atoms, with NPA charges of $q_{\text{Sr}} = +1.715$ and $q_{\text{Al}} = +0.732$. Although there were no notable bonding NBOs between Al and Sr, on initial inspection the HOMO (Figure 3b) mimics a σ -bond along the Al and Sr vector. Scrutiny of the construction of this canonical MO clarifies that the largest component is non-bonding from the Al lone pair (67.1%; LP a combination of AO $3s$ 76.7% and $3p_x$ 19.4 %) with the only other prominent component from a (Si^{Dipp}) nitrogen lone pair (10.8 %). Notably, no NBO associated with Sr significantly contributes to the HOMO. A second order perturbation energy ($\Delta E^{(2)}$) of 29.1 kcal mol⁻¹ was identified with donation from the same Al lone pair to the lone vacancy (LV) of Sr. This latter NBO contains 92.5% of the $5s$ AO, as well as a 7.2 % contribution from d -orbitals, the largest (4.5%) from the $4d_{x^2-y^2}$ Sr AO.

Although the ¹H NMR spectrum of **3^{Sr}** at room temperature in *d*₈-toluene solution presented no indication for asymmetry in the aluminyl-to-strontium interaction, analysis at both mildly elevated and reduced temperatures provided data consistent with a fluxional system. This was most readily apparent from inspection of the *iso*-propyl methine signals arising from the (BDI) and (Si^{Dipp}) ligands. Consistent with time averaged C_{2v} symmetry, at 298 K the respective environments were observed as two broadened signals at δ 3.88 and 2.85 ppm, each resonating with 4H intensity by relative integration. While both signals appeared as well resolved binomial heptets at temperatures above 323 K, below 283 K they were observed to broaden and ultimately resolve as eight well discriminated signals in the range δ 2.5 – 4.5 ppm and of the same 1H intensity by relative integration (Figure S15). Although no precise coalescence temperature could be confidently identified, we suggest that these observations indicate the persistence of a solution structure analogous to that identified in the solid state, but which is also free to pivot at the aluminium centre allowing the (Si^{Dipp}) aryl substituents to interact alternately with the strontium centre.

Mindful of the reactivity of **3^{Ca}** summarised in Scheme 1, a slight stoichiometric excess of THF was added to a toluene solution of **3^{Sr}**. In contrast to the notably immediate reaction of **3^{Ca}**, analysis by ¹H NMR spectroscopy provided no evidence of reaction at room temperature beyond an increase in resolution of the signals assigned to **3^{Sr}**. Repetition of the experiment with heating at 100 °C for 16 hours, however, resulted in the complete consumption of **3^{Sr}**, which occurred through the generation of the known homoleptic derivative, [(BDI)₂Sr],⁴⁰ which was identified alongside a predominant new species, **5**. It was subsequently observed that similar spectra were also obtained by heating a toluene solution of **3^{Sr}** under identical thermal conditions. Although a pure bulk sample of **5** could not be obtained, its constitution was established by a further X-ray diffraction analysis performed by mechanical separation of a single crystal from the mixture of products isolated after storage of the reaction solution at -30 °C. The resultant structure (Figure 4) identified **5** as a homoleptic strontium bis-hydrido(*m*-tolyl)aluminato arising from Al-centred activation of a *meta*-C-H bond of the toluene solvent and, consistent with the

concurrent formation of [(BDI)₂Sr], dismutation from the initial heteroleptic constitution of the β -diketiminato reagent **3^{Sr}**. The centrosymmetric structure of **5** features two aluminate anions that provide the entirety of the strontium coordination environment, interacting through a twofold combination of Al- μ -H-Sr interactions and η^6 - π -arene engagement (Sr...C_{cent} 2.702 Å) with a single Dipp substituent of each (Si^{Dipp}) ligand. We note that a similar stereoelectronic preference for *meta*-selective C-H activation of toluene and various other monoalkylated benzenes has been previously described for both **1** and Yamashita's potassium dialkylaluminyl, [(CH₂(Me₃Si)₂C)₂AlK].^{57,58}

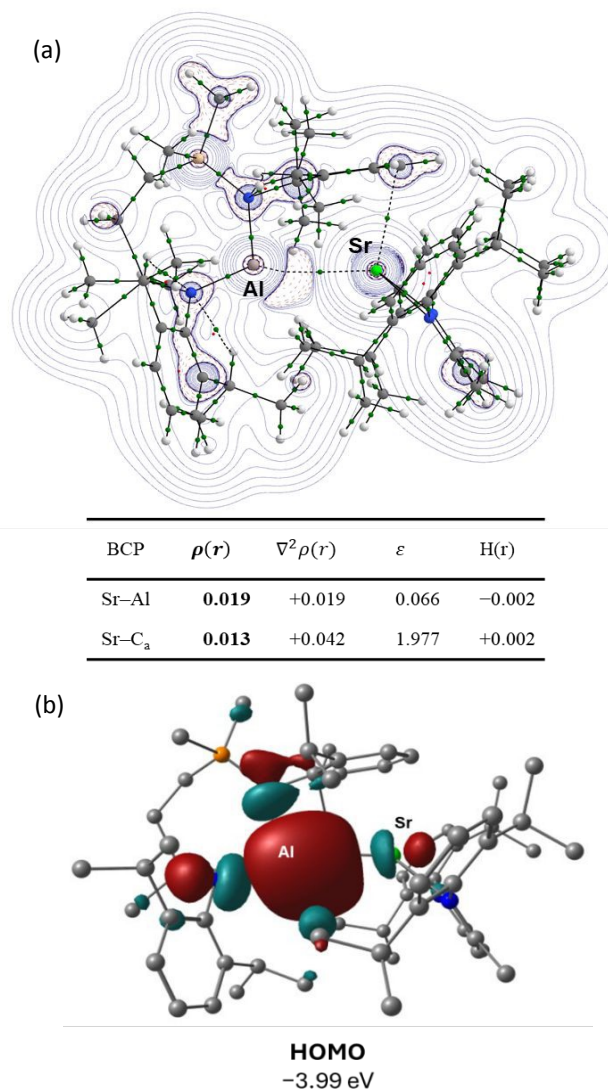


Figure 3. Electronic structure data for **3^{Sr}** (BP86/BS2, see ESI for full details) a) QTAIM molecular graph of **3^{Sr}**. The Laplacian of the electron density ($\nabla^2\rho(r)$) contours are computed in the {Al-Sr-N_{Al}} plane with bond critical points (BCPs) shown as small green spheres. BCP electron density ($\rho(r)$; ea_0^{-3}), Laplacian of the electron density ($\nabla^2\rho(r)$; ea_0^{-5}), ellipticity (ϵ) and total energy density (H(r)) are tabulated beneath. b) Canonical HOMO of **3^{Sr}**.



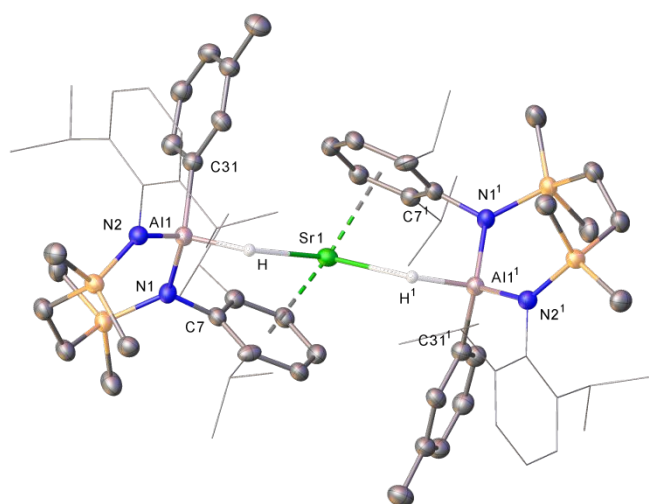


Figure 4. Molecular structure of compound **5** with displacement ellipsoids at 30%. For clarity, hydrogen atoms, apart from the aluminate hydride, are omitted. Similarly, Dipp substituents not involved in π -arene interactions and all *iso*-propyl substituents are displayed as wireframe. Selected bond lengths (Å) and angles (°): Al1-N1 1.889(5), Al1-N2 1.856(5), N2-Al1-N1 113.9(2). Symmetry operations to generate equivalent atoms: $1-x, +y, 3/2-z$.

It has neither proved possible to further deconvolute the processes leading to compound **5** nor to identify whether Schlenk-type redistribution occurs prior to or subsequent to activation of the solvent. The absence of definitive evidence for the solution speciation responsible for the formation of **5**, therefore, dissuades us from further theoretical analysis. The *meta*-specificity of the toluene activation, however, is evocative of several earlier studies of concerted S_NAr Al(I)-to-arene addition implicating *s*-block-assisted assembly of a Meisenheimer-type transition state that evolves by C-to-Al hydride migration.^{35,57-59}

Despite the apparent similarity of its electronic structure to its calcium analogue, **3^{Sr}** evidently presents significantly divergent reactivity toward THF. The thermal and configurational stability displayed by **3^{Sr}** in toluene, however, leads us to suggest that the effect, if any, of ether solvent is to merely facilitate the solution redistribution of the heteroleptic strontium β -diketiminato rather than acting as a direct participant in any alumanyl-centred reaction. Based on these observations, therefore, we tentatively hypothesise that the generation of **5** results from a combination of the greater lability of Sr toward Schlenk-type redistribution and an enhanced ability of the $[(SiN^{Dipp})Al]^-$ moiety to react as a 'free' alumanyl anion when combined with strontium.⁶⁰ We are continuing to explore this and related reactivity.

Data availability

The data supporting this article have been included as part of the ESI.† Crystallographic data for **4^{Sr}**, **3^{Sr}** and **5** have been deposited at the CCDC under CCDC 2548846-2548848, respectively, and can be obtained from <https://www.ccdc.cam.ac.uk/structures>.

Conflicts of interest

There are no conflicts to declare.

View Article Online

DOI: 10.1039/D6DT01406B

Acknowledgements

The authors gratefully acknowledge EPSRC (EP/X01181X/1, 'Molecular *s*-block Assemblies for Redox-active Bond Activation and Catalysis: Repurposing the *s*-block as 3d-elements') and the University of Bath's Research Computing Group (doi.org/10.15125/b6cd-s854) for their support in this work.

Notes and references

- M. Yamashita and K. Nozaki, in *Synthesis and Application of Organoboron Compounds*, eds. E. Fernandez and A. Whiting, 2015, vol. 49, pp. 1-37.
- J. Hicks, P. Vasko, J. M. Goicoechea and S. Aldridge, *Angew. Chem. Int. Ed.* 2021, **60**, 1702-1713.
- M. P. Coles and M. J. Evans, *Chem. Commun.*, 2023, **59**, 503-519.
- M. P. Coles, Alumanyl Anions. In *Encyclopedia of Inorganic and Bioinorg. Chem.*, R.A. Scott (Ed.), 1-23. <https://doi.org/10.1002/9781119951438.eibc2875>.
- J. Hicks, P. Vasko, J. M. Goicoechea and S. Aldridge, *Angew. Chem. Int. Ed.*, 2021, **60**, 1702-1713.
- E. S. Schmidt, A. Jockisch and H. Schmidbauer, *J. Am. Chem. Soc.*, 1999, **121**, 9758-9759.
- R. J. Baker, R. D. Farley, C. Jones, M. Kloth and D. M. Murphy, *J. Chem. Soc. Dalton Trans.*, 2002, 3844-3850.
- R. J. Schwamm, M. D. Anker, M. Lein, M. P. Coles and C. M. Fitchett, *Angew. Chem. Int. Ed.*, 2018, **57**, 5885-5887.
- L. P. Griffin, M. A. Ellwanger, A. E. Crumpton, M. M. D. Roy, A. Heilmann and S. Aldridge, *Angew. Chem. Int. Ed.*, 2024, **63**, e202404527.
- M. P. Coles, *Chem. Commun.*, 2025, **61**, 15125-15144.
- K. Sugita and M. Yamashita, *Chem. Eur. J.*, 2020, **26**, 4520-4523.
- G. F. Feng, K. L. Chan, Z. Y. Lin and M. Yamashita, *J. Am. Chem. Soc.*, 2022, **144**, 22662-22668.
- P. Zatsepina, T. Moriyama, C. Chen, S. Muratsugu, M. Tada and M. Yamashita, *J. Am. Chem. Soc.*, 2024, **146**, 3492-3497.
- G. Feng, K. L. Chan, Z. Lin and M. Yamashita, *J. Am. Chem. Soc.*, 2024, **146**, 7204-7209.
- J. Hicks, A. Mansikkamaki, P. Vasko, J. M. Goicoechea and S. Aldridge, *Nature Chem.*, 2019, **11**, 237-241.
- C. McManus, J. Hicks, X. L. Cui, L. L. Zhao, G. Frenking, J. M. Goicoechea and S. Aldridge, *Chem. Sci.*, 2021, **12**, 13458-13468.
- L. P. Griffin, M. A. Ellwanger, J. Clark, W. K. Myers, A. F. Roper, A. Heilmann and S. Aldridge, *Angew. Chem. Int. Ed.*, 2024, **63**, e202405053.
- L. P. Griffin, M. A. Ellwanger, A. E. Crumpton, M. M. D. Roy, A. Heilmann and S. Aldridge, *Angew. Chem. Int. Ed.*, 2024, **63**, e202404527.
- A. O'Reilly, A. M. S. Booth, G. W. A. Smith, M. J. Evans, L. Lim, D. A. Pantazis, N. Cox, C. L. McMullin, J. R. Fulton and M. P. Coles, *Chem. Eur. J.*, 2025, **31**, e202500358.
- G. W. A. Smith, A. O'Reilly, C. L. McMullin, J. R. Fulton and M. P. Coles, *Angew. Chem. Int. Ed.*, 2025, **64**, e202512812.
- G. W. A. Smith, S. E. Neale, M. J. Evans, X. N. Li, J. H. Wang, M. G. Gardiner, C. L. McMullin, J. R. Fulton and M. P. Coles, *Chem. Eur. J.*, 2025, **31**, e202404206.
- H. Y. Liu, R. J. Schwamm, M. S. Hill, M. F. Mahon, C. L. McMullin and N. A. Rajabi, *Angew. Chem. Int. Ed.*, 2021, **60**, 14390-14393.
- H. Y. Liu, S. E. Neale, M. S. Hill, M. F. Mahon and C. L. McMullin, *Dalton Trans.*, 2022, **51**, 3913-3924.



24. H.-Y. Liu, S. E. Neale, M. S. Hill, M. F. Mahon and C. L. McMullin, *Chem. Sci.*, 2023, **14**, 2866-2876.
25. H. Y. Liu, J. Kenar, S. E. Neale, M. Garofalo, M. S. Hill, C. L. McMullin, M. F. Mahon and E. Richards, *Organometallics*, 2024, **43**, 3074-3086.
26. J. Hicks, P. Vasko, J. M. Goicoechea and S. Aldridge, *Nature*, 2018, **557**, 92-95.
27. R. J. Schwamm, M. D. Anker, M. Lein and M. P. Coles, *Angew. Chem. Int. Ed.*, 2019, **58**, 1489-1493.
28. R. J. Schwamm, M. P. Coles, M. S. Hill, M. F. Mahon, C. L. McMullin, N. A. Rajabi and A. S. S. Wilson, *Angew. Chem. Int. Ed.*, 2020, **59**, 3928-3932.
29. S. Kurumada, S. Takamori and M. Yamashita, *Nature Chem.*, 2020, **12**, 36-39.
30. K. Koshino and R. Kinjo, *J. Am. Chem. Soc.*, 2020, **142**, 9057-9062.
31. S. Grams, J. Mai, J. Langer and S. Harder, *Dalton Trans.*, 2022, **51**, 12476-12483.
32. R. A. Jackson, A. J. R. Matthews, P. Vasko, M. F. Mahon, J. Hicks and D. J. Liptrot, *Chem. Commun.*, 2023, **59**, 5277-5280.
33. G. M. Ballmann, M. J. Evans, T. X. Gentner, A. R. Kennedy, J. R. Fulton, M. P. Coles and R. E. Mulvey, *Inorg. Chem.*, 2022, **61**, 19838-19846.
34. K. G. Pearce, A. Morales, M. S. Hill and C. L. McMullin, *Chem. Eur. J.*, 2025, **3**
35. H.-Y. Liu, M. S. Hill, M. F. Mahon, C. L. McMullin and R. J. Schwamm, *Organometallics*, 2023, **42**, 2881-2892.
36. H.-Y. Liu, H. T. W. Shere, S. E. Neale, M. S. Hill, M. F. Mahon and C. L. McMullin, *Organometallics*, 2024, **44**, 236-243.
37. J. T. Boronski, L. R. Thomas-Hargreaves, M. A. Ellwanger, A. E. Crumpton, J. Hicks, D. F. Bekis, S. Aldridge and M. R. Buchner, *J. Am. Chem. Soc.*, 2023, **145**, 4408-4413.
38. M. J. Evans, G. H. Iliffe, S. E. Neale, C. L. McMullin, J. R. Fulton, M. D. Anker and M. P. Coles, *Chem. Commun.*, 2022, **58**, 10091-10094.
39. V. C. Gibson, J. A. Segal, A. J. P. White and D. J. Williams, *J. Am. Chem. Soc.*, 2000, **122**, 7120-7121.
40. S. Harder, *Organometallics*, 2002, **21**, 3782-3787.
41. M. H. Chisholm, J. Gallucci and K. Phomphrai, *Chem. Commun.*, 2003, 48-49.
42. S. Sarish, S. Nembenna, S. Nagendran, H. W. Roesky, A. Pal, R. Herbst-Irmer, A. Ringe and J. Magull, *Inorg. Chem.*, 2008, **47**, 5971-5977.
43. A. G. Avent, M. R. Crimmin, M. S. Hill and P. B. Hitchcock, *Dalton Trans.*, 2005, 278-284.
44. A. S. S. Wilson, M. S. Hill and M. F. Mahon, *Organometallics*, 2019, **38**, 351-360.
45. B. Rösch, T. X. Gentner, H. Elsen, C. A. Fischer, J. Langer, M. Wiesinger and S. Harder, *Angew. Chem. Int. Ed.*, 2019, **58**, 5396-5401.
46. B. Maitland, A. Stasch and C. Jones, *Aust. J. Chem.*, 2022, **75**, 543-548.
47. D. B. Kennedy, M. J. Evans, D. D. L. Jones, J. M. Parr, M. S. Hill and C. Jones, *Chem. Commun.*, 2024, **60**, 10894-10897.
48. L. Garcia, M. D. Anker, M. F. Mahon, L. Maron and M. S. Hill, *Dalton Trans.*, 2018, **47**, 12684-12693.
49. L. Garcia, M. F. Mahon and M. S. Hill, *Organometallics*, 2019, **38**, 3778-3785.
50. J. Pahl, S. Brand, H. Elsen and S. Harder, *Chem. Commun.*, 2018, **54**, 8685-8688.
51. J. S. McMullen, A. J. Edwards and J. Hicks, *Dalton Trans.*, 2021, **50**, 8685-8689.
52. R. Mondal, M. J. Evans, D. T. Nguyen, T. Rajeshkumar, L. Maron and C. Jones, *Chem. Commun.*, 2024, **60**, 1016-1019.
53. J. M. Parr, J. Mullins, M. J. Evans and C. Jones, *Chem. Asian J.*, 2026, **21**, e70331.
54. P. Dabringhaus, M. Schorpp, H. Scherer and I. Krossing, *Angew. Chem. Int. Ed.*, 2020, **59**, 22023-22027.
55. M. Schorpp and I. Krossing, *Chem. Sci.*, 2020, **11**, 2068-2076.
56. T. X. Gentner, B. Rösch, K. Thum, J. Langer, G. Ballmann, J. Pahl, W. A. Donaubauer, F. Hampel and S. Harder, *Organometallics*, 2019, **38**, 2485-2493.
57. J. Hicks, P. Vasko, A. Heilmann, J. M. Goicoechea and S. Aldridge, *Angew. Chem. Int. Ed.*, 2020, **59**, 20376-20380.
58. S. Kurumada, K. Sugita, R. Nakano and M. Yamashita, *Angew. Chem. Int. Ed.*, 2020, **59**, 20381-20384.
59. S. Brand, H. Elsen, J. Langer, S. Grams and S. Harder, *Angew. Chem. Int. Ed.*, 2019, **58**, 15496-15503.
60. Aldridge and co-workers have previously commented on the enhanced reactivity of 'naked' boryl and alumanyl anions toward C-H and C-C bonds. See, for example, (a) A. V. Protchenko, P. Vasko, M. A. Fuentes, J. Hicks, D. Vidovic and S. Aldridge, *Angew. Chem. Int. Ed.*, 2020, **60**, 2064-2068; (b) J. Hicks, P. Vasko, J. M. Goicoechea and S. Aldridge, *J. Am. Chem. Soc.*, 2019, **141**, 11000-11003.



The data supporting this article have been included as part of the ESI.† Crystallographic data for 4Sr, 3Sr and 5 have been deposited at the CCDC under CCDC 2548846-2548848, respectively, and can be obtained from <https://www.ccdc.cam.ac.uk/structures>.

View Article Online
DOI: 10.1039/D6DT01406B

